Automated System to Quantify the Behavior of Small Insects in a Four-pointed Star Olfactometer

C. Vigneault, B. Panneton, D. Cormier, G. Boivin

Abstract. *The construction, assembly, and testing of an improved four-pointed star olfactometer are described. Modifications to earlier versions were motivated by the need to automate collection and analysis of data on insect locomotive response to airborne stimuli. A machine vision system capable of resolving small insects (< 1 mm) in arenas of surface area 100,000 times greater than the surface area of the insect was assembled from commercially-available components. A real-time insect positioning and tracking algorithm was developed. A software package for data quality control and computation of insect movement parameters completed the system. Trials conducted with the parasitoid* Anaphes listronoti *(Hymenoptera: Mymaridae) (dimensions 200 by 700 µm) demonstrate that the system provides accurate data on insect locomotive response.* **Keywords.** *Olfactometer, Automation, Image analysis, Tracking, Olfactometer, Behavior, Insect, Parasitoid.*

The four-pointed star olfactometer, whose shape is shown as figure 1, was originally developed for the study of insect responses to pheromones by Pettersson (1970). The olfactometer is based on the formation of four distinct regions of airflow, separated by transition zones, in a single arena where the insect is free to move. These flow regions arise from the combined effects of the curved edges and principal flow streamlines from the star points to the central hole. The stimulus or stimuli are applied from one or more of the star points. The flows may be maintained by a vacuum pump acting on the central hole and drawing on the four star point outlets or by applying positive pressure to the star points. The degree of exclusivity of each region to stimuli from other star points depends on the magnitude, steadiness, and equivalence of the flow velocities in each axis segment. Compared to Y-shaped (Lecomte and Thibout, 1984), wind tunnel (Grasswitz and Paine, 1993) and tube (Cortesero et al., 1993; Mochizuki et al., 1989) olfactometers, this design gives several important methodological advantages to the experimenter. As discussed by Vet et al. (1983) the star configuration permits observation of insect response to up to four airborne stimuli (or four concentrations of the same stimulus) at a time and reduces the number of individuals to be tested for a given level of statistical certitude.

Vet et al. (1983) improved the original design by including: (1) a sensitive airflow control system to provide sharper boundaries in the odor fields of the arena; (2) an inlet system allowing solid or liquid sources of odor; and (3) catching vials for testing individual insects. Although they eliminated the need for an observer during the testing periods by using a video camera to obtain a permanent record, quantification of the displacements was done by manual transcription of visual observations of the recorded tapes. This tedious procedure is common to behavioral research, yet can be fully automated using electronic image analysis techniques based on commercially available components and custom software.

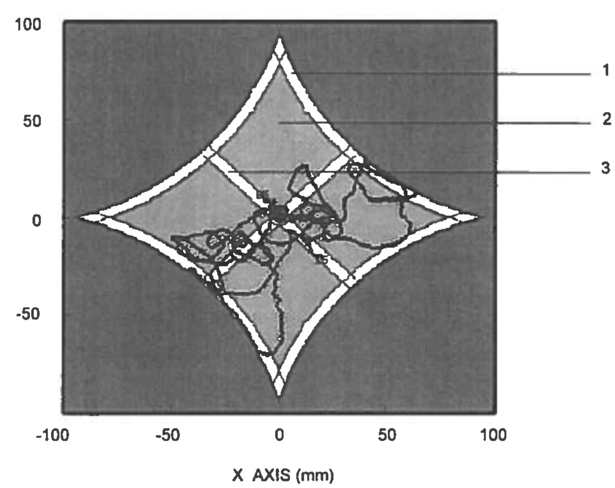

Figure 1–Schematic of four-pointed star olfactometer indicating boundary zones (no. 1), major sectors (no. 2), transition zones (no. 3), and with an example insect path from system superimposed.

Article was submitted for publication in March 1996; reviewed and approved for publication by the Information & Electrical Technologies Div. of ASAE in April 1997.

This is a contribution 335/97.05.04R of the Horticultural Research and Development Centre, Agriculture and Agri-Food Canada, St-Jean-sur-Richelieu, PQ. Mention of product or company names is for presentation clarity and does not imply endorsement of the product or company by the authors or Agriculture and Agri-Food Canada or McGill University, or exclusion of other products that may also be suitable.

The authors are **Clément Vigneault,** ***ASAE Member Engineer***, Eng., Ph.D., **Bernard Panneton,** ***ASAE Member Engineer***, Eng., Ph.D., **Guy Boivin**, Entomologist, Ph.D., Horticultural Research and Development Centre, Agriculture and Agri-Food Canada, Saint-Jean-sur-Richelieu, PQ, Canada; and **Daniel Cormier**, Entomologist, Graduate Student, Department of Natural Resource Sciences, Macdonald Campus, McGill University, Sainte-Annede-Bellevue, PQ, Canada H9X 3V9. **Corresponding author:** Clément Vigneault, Horticultural Research and Development Centre, Agriculture and Agri-Food Canada, Saint-Jean-sur-Richelieu, PQ, Canada J3B 3E6; tel: (514) 346-4494, ext. 213; fax: (514) 346-7740; e-mail: <vigneaultc@em.agr.ca>.

OBJECTIVES

The main objective of this study was to automate transcription of the visual images of insect to digital form suitable for computer calculations of relevant quantitative displacement parameters. The sub-objectives were: (1) to modify the olfactometer and accessories to obtain a clearer image, and in particular, to obtain a clear image of small parasitoid insects in arenas about 100,000 times greater than the surface area of the insect; (2) to develop a search algorithm to position the insect; (3) to optimize the data recording frequency; and (4) to develop an analytical method to characterize the insect displacement and quantify its behavior. The whole system was evaluated using *Anaphes listronoti* (Hymenoptera: Mymaridae), whose approximate dimensions are 200 × 700 µm, as well as with larger species.

MATERIALS AND METHODS

DESCRIPTION OF THE OLFACTOMETER

The olfactometer built for this study was designed principally to improve the clarity of the image while preserving well-segregated airflow sectors. Although quite similar in concept to the olfactometer described by Vet et al. (1983), the materials, design, and operating modes of the olfactometer itself were substantially modified as described below. The eleven-piece assembly consisted of four layers of Plexiglas, one layer of aluminum, two gaskets, and four quick-clamps (fig. 2). The construction was as follows:

A 140 mm square was inseted 6 mm from the bottom surface of a 10 mm thick, 184 mm square aluminum plate. The star shape was then cut out of the inset square (fig. 2, no. 1). The inset square bottom was plugged with a 6 mm thick, 139.8 mm square Plexiglas plate (fig. 2, no. 2). This Plexiglas piece was the arena floor on which the insect moved. Two, 184 mm square Plexiglas plates, 12.7 mm thick, were placed so as to cover the whole top and bottom surfaces of the sculpted aluminum plate, leaving a star-shaped arena 4 mm in depth (fig. 2, no. 3 & no. 4). Both the top and bottom Plexiglas plates were grooved about 15 mm from the edge and fitted with 3 mm thick black rubber o-rings to provide an airtight seal upon complete assembly (fig. 2, no. 5). The four corners of the aluminum plate (fig. 2, no. 1) had 5 mm diameter holes drilled in the direction of the diagonal to provide airflow access to the arena. A 9 mm diameter exhaust hole was drilled into the center of the top Plexiglas cover. This method of construction ensured that no imperfections in the Plexiglas due to machining will be in the field of view of the camera, except near the drilled center hole.

The assembly was then placed on a 370 mm square Plexiglas plate (fig. 2, no. 6), 10 mm thick, to which four quick-clamps were screwed to hold the arena assembly tightly in place (fig. 2, no. 7). The quick-clamps also reduced the time required to dismantle and clean the apparatus between experiments. A semi-opaque Lexan plate (4 mm thick) was placed under the assembly to diffuse the circular neon light source (40 W) to provide a more even light distribution. The choice of placing the light source beneath, rather than above the arena floor, was made to improve the contrast between the background and the insect as seen by an overhead camera.

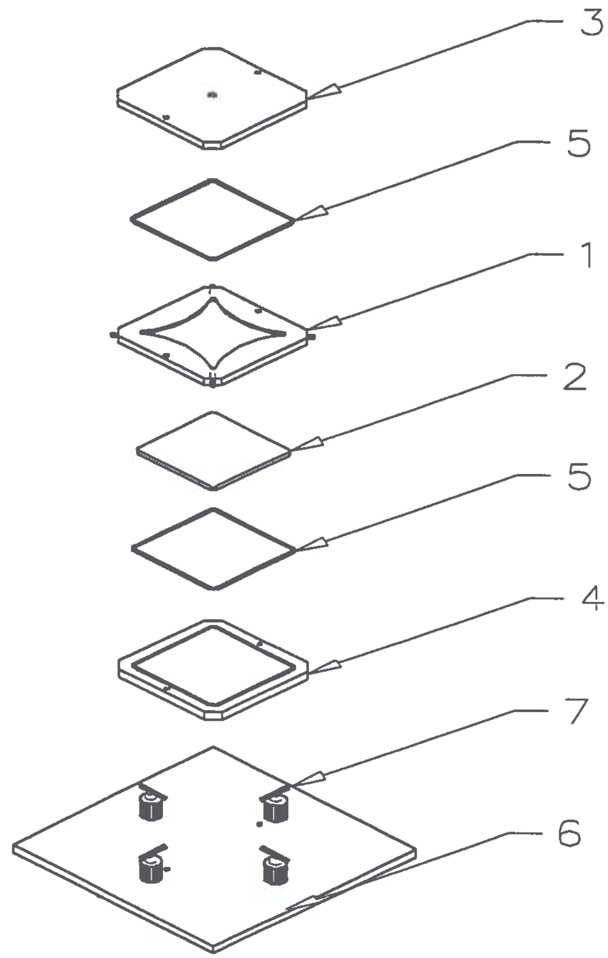

Figure 2–Olfactometer assembly: middle aluminum plate (no. 1), middle Plexiglas back plate (no. 2), top and bottom Plexiglas plates (no. 3-4), gaskets (no. 5), and quick-clamps (no. 7) on a Plexiglas plate (no. 6).

Positive pressure was supplied by a canister of compressed air connected with Tygon tubing to a 2 L Erlenmeyer flask half-filled with water to maintain humidity. A 50 mm long, 16 µm capillary tube was set between the pressure regulator and the Erlenmeyer to smooth the pressure fluctuations caused by the on-off mode of the regulator. The Erlenmeyer was connected to a 4-way junction and four micro-needle controlled flowmeters. Tubing linked the flowmeters to the corners of the olfactometer. Flasks containing airborne stimuli can be inserted in one or more of the paths to the corners, depending on the experimental objectives. The complete setup is shown in figure 3.

PRELIMINARY TESTING

A number of preliminary tests were conducted to ensure proper functioning of the olfactometer. First, airtightness of the olfactometer was evaluated using a method similar to the one described by Vigneault et al. (1992a) for a closed container. All orifices of the olfactometer were plugged and the unit was pressurized to 125 Pa under constant temperature (23°C). The inside pressure was monitored for the next 15 min and corrected for variations in barometric pressure. The four quick-clamps were tightened to prevent

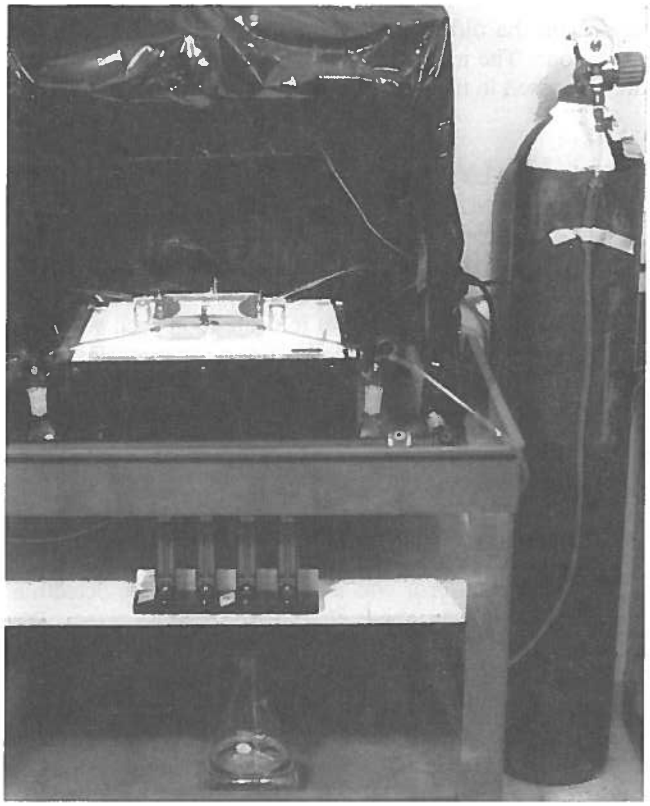

Figure 3–Experimental setup: olfactometer, camera, light source, and airflow system.

the pressure from dropping to lower than 25 Pa within the next 5 min period. This pressure drop corresponds to one air change in 3.5 days (Vigneault et al., 1992a), which is about 400,000 times less than the air changes due to the airflow rate that would be used during actual operation. Thus, infiltration through the joints of the olfactometer can be neglected.

The 300 mL/min airflow rate suggested by Vet et al. (1983) for a 10 mm deep cavity was reduced to produce sharp boundaries between the four air flow fields in the 4 mm deep chamber that was built for this study. Ammonium chloride (NH_4Cl) smoke tests described by Vet et al. (1983) were performed using airflow rates of 300, 150, 75, and 37 mL/min. The results of these tests demonstrated that the sharpest boundaries between the air fields were obtained at a flow rate of 150 mL/min. Boundaries were slightly curved and smoke was seen 5 mm inside the two adjacent zones. Therefore, transition zones were about 10 mm wide at this flow rate.

The focal plane of the camera was adjusted to the mid-height of the cavity using the focusing method described by Vigneault et al. (1992b). Thus, the insect could not be more than 2 mm from the focal plane whether it moved along the floor or ceiling of the arena. The focus was sufficiently sharp in this range to ensure that the insect could always be detected by the machine vision system to be described.

Insect Tracking and Positioning System

The insect tracking and positioning system used a Solid-State Charged-Coupled-Device (CCD) black and white camera (Panasonic WV-BD400) to provide a video signal to an OCULUS-300 digitizing board installed in a 12 MHz IBM-AT compatible personal computer. The system can map the images to an array of 480 × 512 square pixels up to 30 times/s in real time with 8 bits of resolution per pixel. This degree of resolution permitted discrimination of 256 gray levels coded from 0 to 255. It should be noted that a level of 0 is the darkest while a level of 255 is maximum light intensity that the CCD can measure. A 75 mm lens with +3 close-up kit were used, giving a system resolution of 250 ± 5 µm/pixel side. This was about one-third the dimensions of the micro-insect *Anaphes listronoti* (200 µm × 700 µm). The digital data were recorded and also displayed in real time on a monitor for the operator.

Prior to insertion of the insect and actual tracking, the operator initiated a scan of the whole field. The gray level of each pixel was stored in memory to serve as a reference map. Once the insect was placed in the olfactometer, subsequent digitized maps were subtracted from the reference map, the difference map being used for the positioning and tracking (PT) algorithm. This subtraction procedure eliminated unwanted signals due to dust, nonuniform lighting, or imperfections in the Plexiglas plates. It also simplified the PT algorithm by eliminating the need to discriminate between dark pixels associated with the olfactometer's structure and dark pixels associated with the presence of the insect. The result of image subtraction, when regenerated as an image on the monitor, was a bright dot representing the insect on a dark background. Figure 4 shows how the image subtraction technique effectively inverts the peak associated with insect position from dark to bright by subtracting the incoming image from the reference map. During the subtraction a positive value (fig. 4; gray level = 33) resulted because the gray level of the pixels representing the insect (fig. 4; gray level = 161) was lower than the ones of the background in the reference map (fig. 4; gray level = 194). Any negative value was being replaced by a zero value. The operator must also specify a threshold gray level (for *A. listronoti* = 20) to the system software so that it may

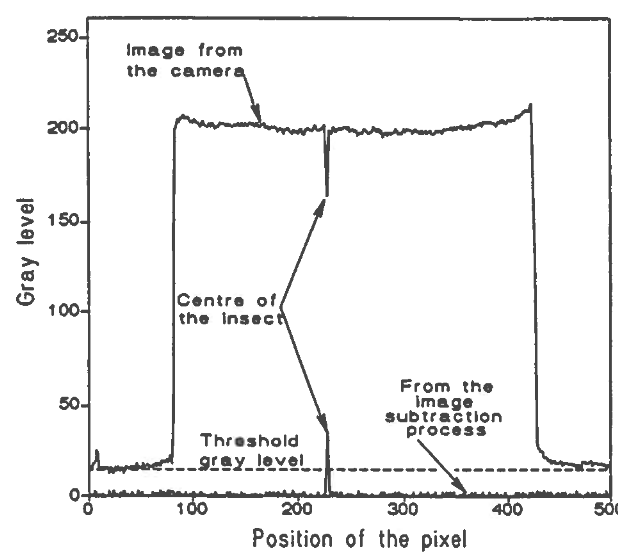

Figure 4–Image subtraction: reference signal shown with direct camera signal when centered on insect and inverted off-set signal obtained from subtraction method.

discriminate between minor noise peaks and peaks due to insect presence (fig. 4).

In order to locate the insect, the operator used an indicator to identify a starting point on the screen monitor. For *Anaphes listronoti*, the search process was initiated on a sector of 25 × 25 pixels with the starting point at the center. Relative to figure 5, the image was scanned row by row starting from the top of the sector. If no pixel with a subtracted gray index greater than the threshold gray level (e.g., *A. listronoti* = 20) was detected, the scan was redone on the same sector for the next three images. If it was still not found, the scan was done on a sector twice as large. If again, no significant pixel was detected, the scanned sector was again enlarged, and so on until a significant pixel was detected. Once this occurs (fig. 5; pixel 346, 200), a scan was made on a 5 × 4 pixel sector with the starting point being two pixels back and one row up from the detected point. Zooming out in this way ensured that an insect of dimensions 200 × 700 μm will be totally included in the 20 pixel scan (bold bordered region in fig. 5). In order to be certain that the significant pixel was due to the presence of the insect and not due to an isolated error, the sum of the gray levels in the 20 pixel region was computed. If it was greater than five times the threshold gray level, the system recognized that the insect was in the region, otherwise the search continued. For insects of other dimensions, the scanning parameters must be adjusted.

The position specified and stored in the tracking file along with the time (± 0.001 s) was the coordinate determined by calculating the first-order moment of the gray levels of the 20 pixels. Although the system can provide up to 13 records/s on the 12 MHz computer, the insect may be "lost" from time to time, either due to rapid displacements (flitting), or due to being hidden at or in the periphery of the exhaust hole where contrast was poor. False detections may also occur due to the settling of dust

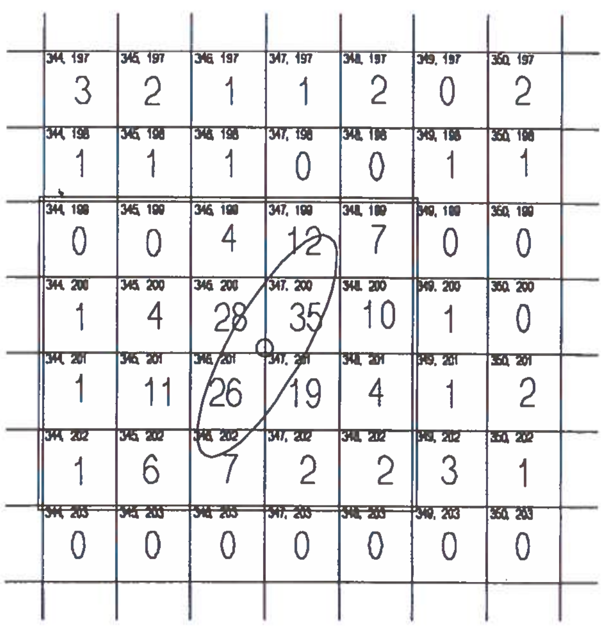

Figure 5–Example of a pixel array with an insect present (oval shape). Dark bordered region is zoom-out region after detection of first pixel with gray level above threshold. Scanning is from top, left to right.

or dirt on the olfactometer after the background scan has been done. The methods used to overcome these problems are discussed in the following section.

Data Analysis

Pre-processing

The pre-processing software has been designed for quality control of a given PT data set. The first step was a routine that identified occasions on which the insect was "lost" and the time required to relocate it on each occasion. Based on this information, the operator may decide to discard the data set altogether. Clearly, if the insect was "lost" on too many occasions and/or for too great a percentage of time, the movement parameters that could be computed would be much less reliable, unless the "loss" periods correspond mainly to time spent near the exhaust hole (i.e., position and potential displacement were essentially known).

One cause of error was associated with false detection, i.e., detection of an object that looked like an insect. Dirt particles can be the source of false detection. The number of false detections can be minimized by careful experimentation but cannot be avoided completely given the searching algorithm that was used. When a false detection occurred, the measured path displays a kink of arbitrary amplitude. Such kinks could be removed manually but this was tedious. Instead, a low pass filter was applied to the data.

A digital filter cannot be applied directly to the original data because the time increment used to digitize the insect path was not fixed but varies as the efficiency of locating the insect varies. This problem can be solved by redigitizing the insect path at a fixed time interval assuming that the insect moved at constant speed and on a straight line path between two successive points in the original time series. This process definitely destroyed the high frequency content of the measured path. However, as shown on figure 6, the contribution to the total variance was at least two decades down for frequencies roughly above 0.5 Hz. Given a digitizing frequency of about 6 Hz and a redigitizing frequency of 4 Hz, it was clear that the redigitizing process did not alter the data significantly.

A digital recursive filter of the Butterworth type was used (Bendat and Piersol, 1971). The filter gain curve

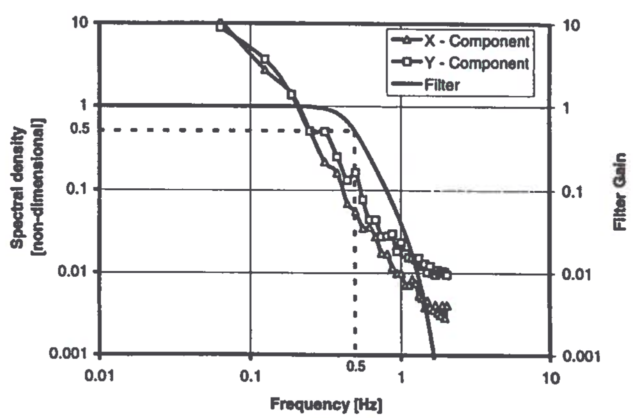

Figure 6–Low-pass filter gain function and spectral densities of the X and Y components of insect displacement (*Anaphes listronoti*).

shown in figure 6 shows a cutoff (half-power point) frequency of 0.5 Hz. A cutoff frequency of 0.5 Hz was high enough to preserve virtually all the significant variability in the data (fig. 6). Further, at the Nyquist frequency (2 Hz), the filter gain was on the order of 10^{-9}. Such a gain ensured that the amplitude of any kink in the path induced from false detection was attenuated well below the pixel level.

The use of a low-pass filter was also useful for identifying the occasions where the insect stopped. For a small insect like *Anaphes listronoti* with a width on the order of the pixel, some noise in the coordinate data was to be expected. Computation of insect speeds amplify this noise (Bendat and Piersol, 1971) and makes the identification of stops more difficult. Filtering the data solved this problem.

Data Reduction

The path of the insect within the olfactometer can be described using a number of statistics. By design, the olfactometer is not a spatially homogeneous field. Accordingly, statistics computed over the whole useful area of the olfactometer are not appropriate. For this reason, the pixel representation of the instrument working area was divided into seven zones.

Figure 1 shows a typical insect path (thick black line) within the useful area of the olfactometer (light gray and white areas, star shaped area). The periphery of the olfactometer was one zone (fig. 1, no. 1 white zone). Its width was defined by the user to isolate the wall-following behavior that can be observed on two segments of the path. A circle in the center of the representation with radius equal to the radius of the gas exit hole defined another zone. In this zone, the insect behavior was dominated by the geometry since the airflows from the four entrance ports mixed in this area. Four main zones were associated with the four entrance ports (fig. 1, no. 2 light gray areas). The boundaries between these four zones were grouped in a separate zone (fig. 1, no. 3). The width of the boundary (or concentration transition) zone was about 10 mm at a flow rate of 150 mL/min according to the smoke test; however, the width may be defined by the operator to smaller or larger values according to the relevance to the experimental hypothesis.

For each zone, except the one at the center of the instrument, the following statistics were computed: mean speed, total length of the path, total time spent in the zone, mean kinetic energy, the average turning rate, and the turn bias. The turning rate was the absolute value of the derivative of the path azimuth with respect to time. The turn bias was the average of the derivative of the path azimuth with respect to time. A positive turn bias indicated that left turns dominate. When the insect exited the olfactometer from one of the entrance ports, it was said that a final choice was made. The sector corresponding to the port where final choice occurred was identified and the time from the first instant the insect entered this area to the instant where it exited through the port, was reported. These statistics were also pooled over all the zones and computed. The main use of the overall statistics was as a cross-check of the data. Finally, statistics on stops in insect displacement were computed for each of the four zones corresponding to the four gas entrance ports. A stop was defined as a period of time over which the insect center of gravity has not moved. In order for the software to discriminate between a stop and actual displacement, it was necessary to define a threshold speed under which displacement was not likely to have occurred. This is because non-displacement movements (such as shaking of antenna, lifting of leg, turning of head) cause small changes in the pixel gray levels that were interpreted as change in position by the software. This can be done from the resulting speed histogram associated with times of no displacement and selecting a threshold speed (e.g., 2 or 3 standard deviations). Stop data were classified according to the duration of the stop. A histogram was constructed for each of the four zones. The data analysis program has several data output options (tables and graphs) that are useful for detailed analysis and debugging.

Discussion and Conclusion

The images produced using the new olfactometer were of excellent quality. The contrast between the insect and the background was better than required for position tracking. Even if the contrast was reduced when recording on a video tape, it was still good enough to perform image analysis. When the depth of the apparatus was 4 mm and the camera's focal plane centered at mid-depth of the olfactometer cavity, the insect was recognizable by the image analysis system even if it was on the floor or ceiling of the olfactometer cavity.

As shown in figure 1, the system can accurately track and record the position of a small insect 200 μm × 700 μm (0.14 mm^2) on a 14 000 mm^2 surface. Larger insects can also be tracked after suitable adjustments of the cavity depth and parameters of the search algorithm. The stored tracking data can be used to calculate a wide variety of indicators of movement.

The system consisting of a four-pointed star olfactometer and software-controlled positioning, tracking, and recording hardware represents a step forward for insect behavioral research. The setup is suitable for tracking small and large insects in a relatively large arena with a high degree of temporal and spatial resolution and little human intervention. While the system was developed in the context of studying response to airborne stimuli, it should be easily applicable to other types of behavioral research.

Acknowledgments. The authors wish to acknowledge the assistance of Mr. Patrick Lemonde for building the olfactometer, and the help of Mr. Peter Alvo in revising the manuscript.

References

Bendat, J. S. and A. G. Piersol. 1971. *Random Data: Analysis and Measurement Procedures*. New York, N.Y.: Wiley Interscience.

Cortesero, A. M., J. P. Monge and J. Huignard. 1993. Response of the parasitoid *Eupelmus vuilleti* to the odours of the phytophagous host and its host plant in an olfactometer. *Entomologia Experimentalis et Applicata* 69(2):109-116.

Grasswitz, T. R. and T. D. Paine. 1993. Effect of experience on inflight orientation to host-associated cues in the generalist parasitoid *Lysiphlebus testaceipes*. *Entomologia Experimentalis et Applicata* 68(3):219-229.

Lecomte, C. and E. Thibout. 1984. Étude olfactométrique de l'action de diverses substances allélochimiques végétales dans la recherche de l'hôte par *Diadromus pulchellus* (Hymenoptera, Ichneumonidae). *Entomologia Experimentalis et Applicata* 35(3):295-303.

Mochizuki, A., Y. Ishikawa and Y. Matsumoto. 1989. Olfactory response of the larvae of the onion fly, *Hylemya antiqua* Meigen (Diptera: Anthomyiidae) to volatile compounds. *Appl. Entomol. and Zoology* 24(1):29-35.

Pettersson, J. 1970. An aphid sex attractant. 1. Biological studies. *Entomol. Scandinavica* 1(1):63-73.

Vet, L. E. M., J. C. van Lenteren, M. Heymans and E. M. Meelis. 1983. An airflow olfactometer for measuring olfactory responses of hymenopterous parasitoids and other small insects. *Physiol. Entomol.* 8(1):97-106.

Vigneault, C., V. Orsat, B. Panneton and G. S. V. Raghavan. 1992a. Oxygen permeability and airtightness measuring method for breathing bags. *Can. Agric. Eng.* 34(2):183-187.

Vigneault, C., B. Panneton and G. S. V. Raghavan. 1992b. Image analysis of 3-D clouds of bubbles. *Can. Agric. Eng.* 34(4):347-352.